Supplementary Materials for

Large-scale photovoltaic solar farms in the Sahara affect solar power generation potential globally

Jingchao Long[1,2,6,7*], Zhengyao Lu[2*], Paul A. Miller[2], Julia Pongratz[3], Dabo Guan[4], Benjamin Smith[5,2], Zhiwei Zhu[8], Jianjun Xu[1,6], Qiong Zhang[9]

[1]*College of Ocean and Meteorology/South China Sea institute of marine meteorology (SIMM), Guangdong Ocean University, Zhanjiang, China*
[2]*Department of Physical Geography and Ecosystem Science, Lund University, Lund, Sweden*
[3]*Department of Geography, Ludwig Maximilian University of Munich, Munich, Germany*
[4]*Department of Earth System Science, Tsinghua University, Beijing, China*
[5]*Hawkesbury Institute for the Environment, Western Sydney University, Penrith, Australia*
[6]*CMA-GDOU joint laboratory for Marine meteorology, Guangdong Ocean University, Zhanjiang, China*
[7]*Key Laboratory of Climate, Resources and Environment in Continental Shelf Sea and Deep Sea of Department of Education of Guangdong Province, Guangdong Ocean University, Zhanjiang, China*
[8]*School of Atmospheric Sciences, Nanjing University of Information Science and Technology, Nanjing, China*
[9]*Department of Physical Geography and Bolin Centre for Climate Research, Stockholm University, Stockholm, Sweden*

Corresponding author: Zhengyao Lu (zhengyao.lu@nateko.lu.se); Jiangchao Long (longjc@gdou.edu.cn)
* These authors contributed equally

This PDF file includes:

Supplementary Figure 1 to 7
Supplementary Table 1 to 2

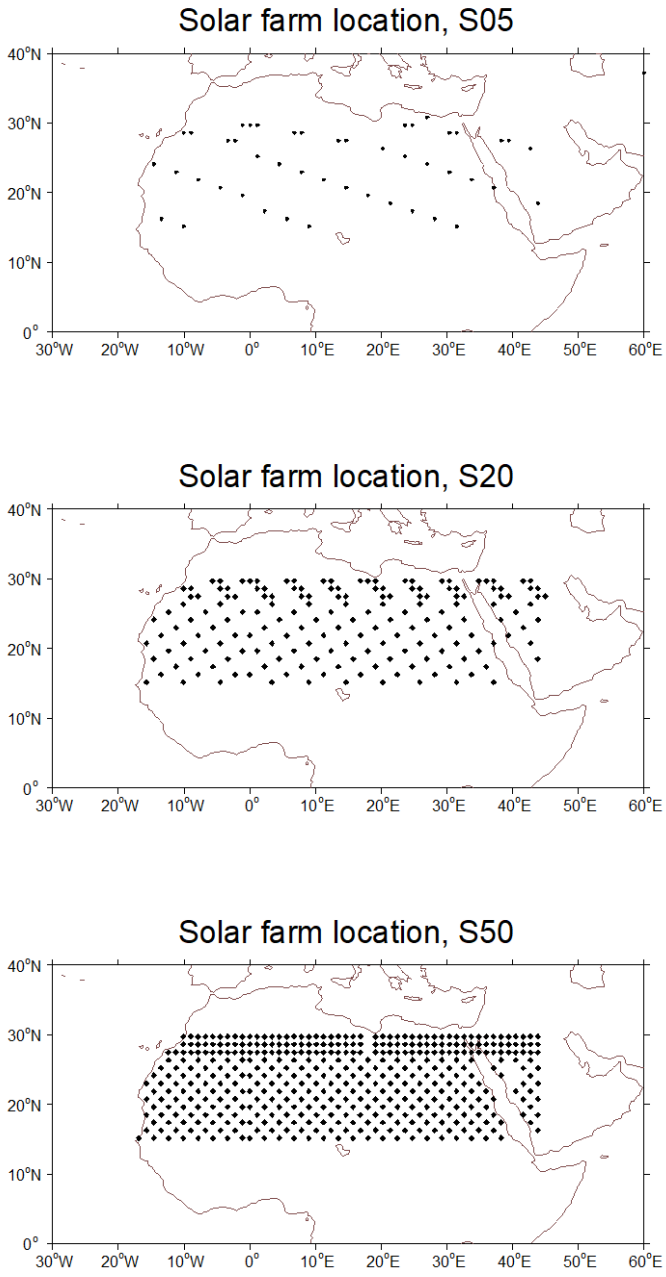

Supplementary Figure 1

The location of Sahara solar farms in S05, S20 and S50 (black dots) as prescribed in model gridcells. One of every 20, 5 and 2 land gridcells North Africa (15-30°N, 20°W-45°E) are modified in S05, S20 and S50, and results in the "checkerboard" spatial patterns of solar farms. Note that there is irregularity near northern boundary of the solar panel area and along 0° longitude line due to the irregular model land gridcell.

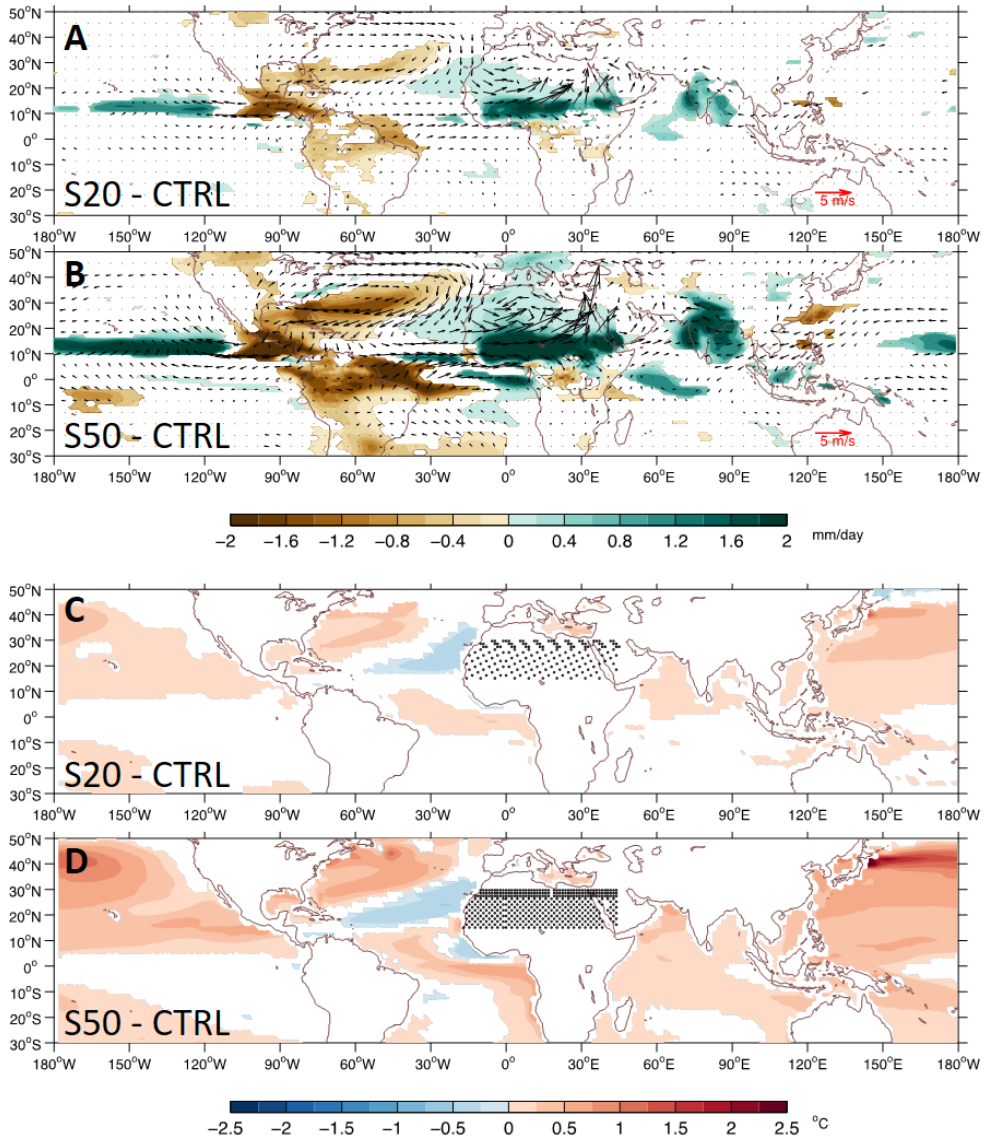

Supplementary Figure 2

Modeled June-July-August mean (A)-(B) precipitation and 925 hPa wind and (C)-(D) annual mean SST response for S20−CTRL, S50−CTRL. All anomalies shown exceed 95% significance level by *t* test. Black dots show model gridcells prescribed as solar panels for S20 and S50.

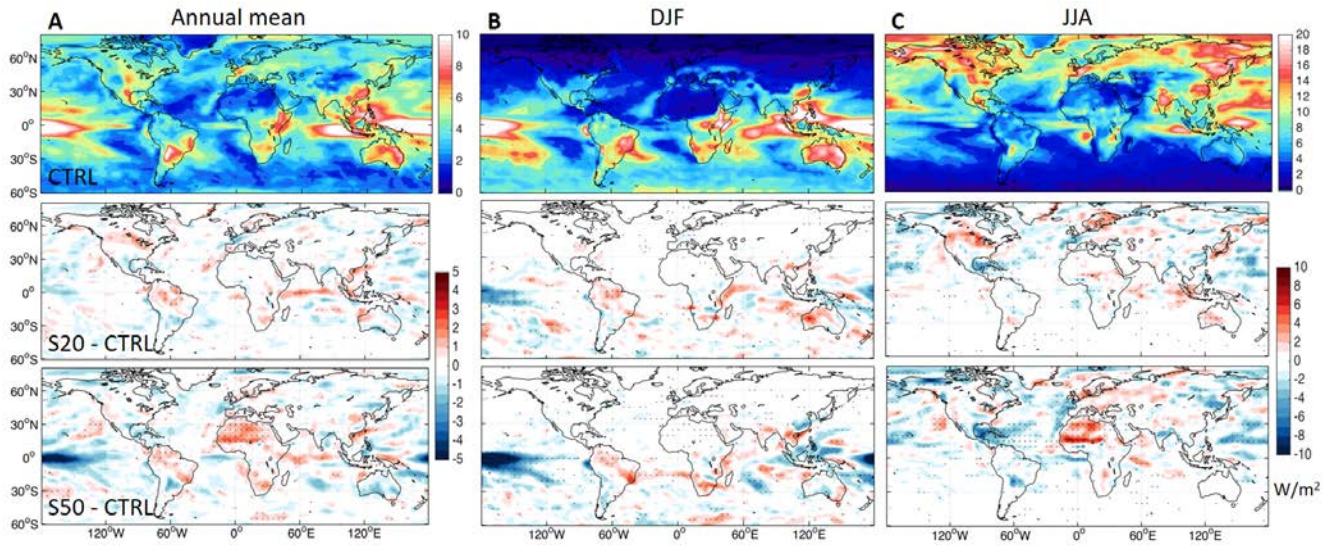

Supplementary Figure 3

SSRD interannual variability (interannual standard deviation) changes for (A) annual mean, (B) DJF mean and (C) JJA mean. The middle and lower panels show results of S20-CTRL and S50-CTRL.

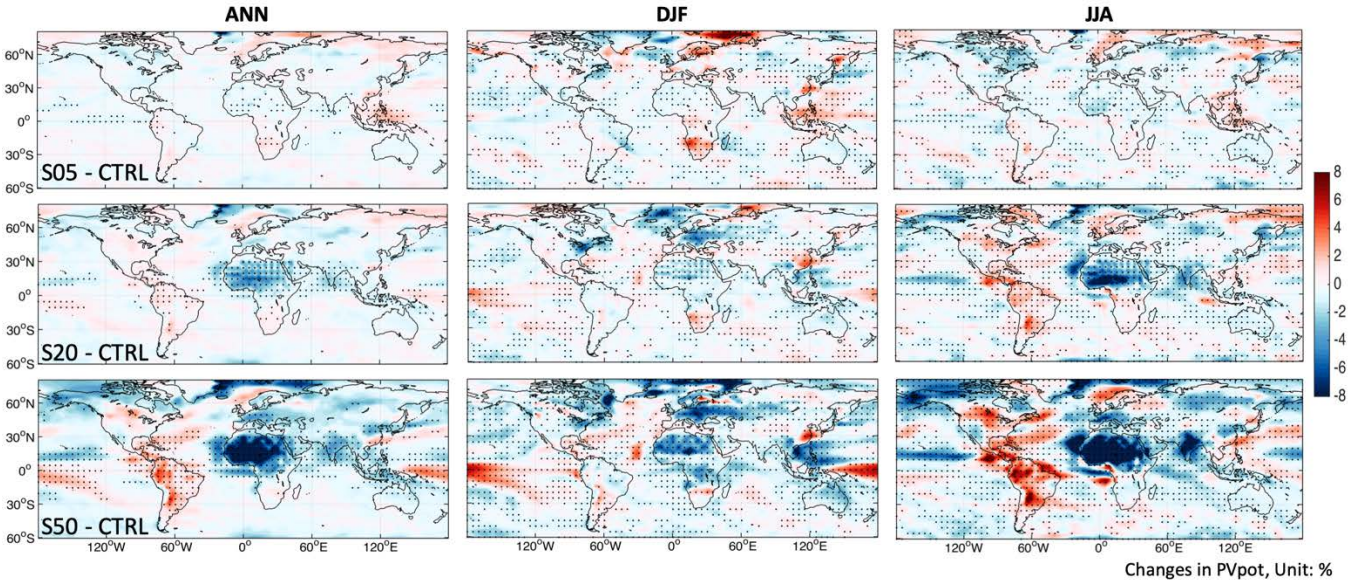

Supplementary Figure 4

Same as Fig. 3 but with 9-point running smooth applied to the time dimension (interannual variability removed). In this way, while the mean differences are not changed, the *t test* mainly tests the significant differences on decadal or longer timescales. The regions showing significant differences are much larger than those in Fig. 3, which implies interannual timescale variability contributes greatly to data spread in the simulation time period (60-year).

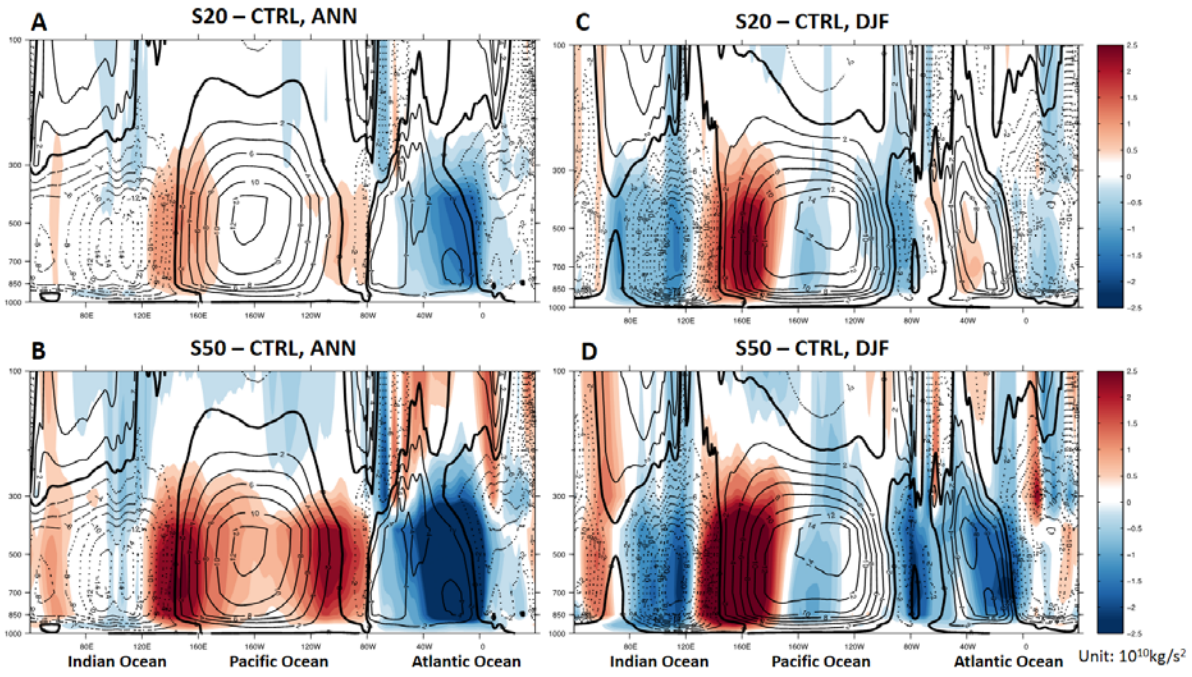

Supplementary Figure 5

Walker circulation changes (shading color) as estimated by stream function. The contours show the mean circulation in CTRL.

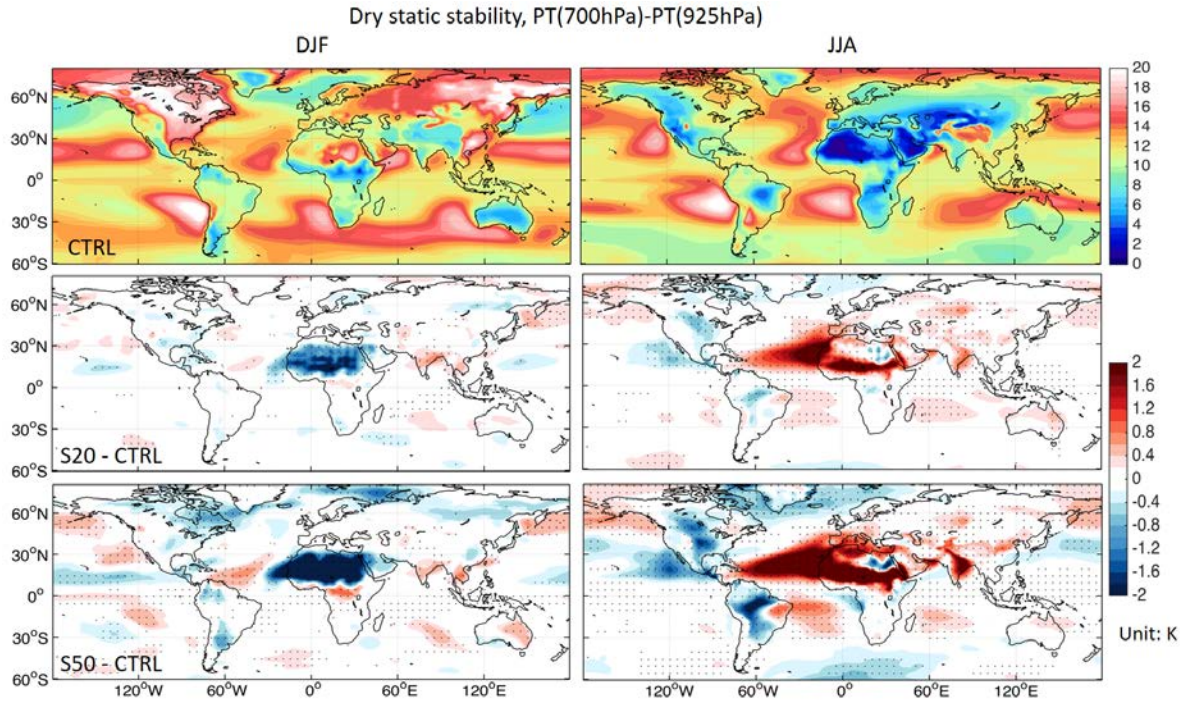

Supplementary Figure 6

Simulated atmospheric dry static stability changes.

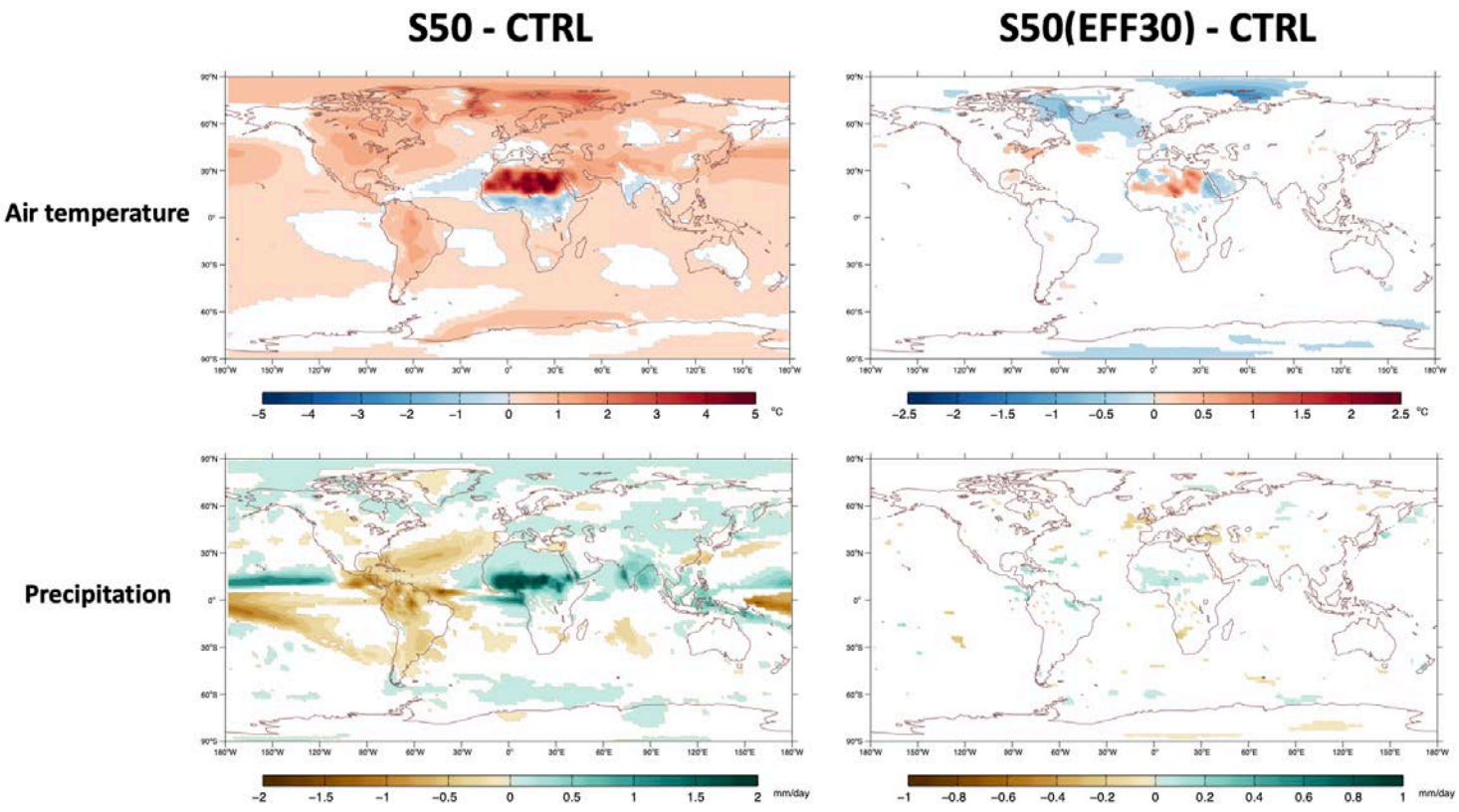

Supplementary Figure 7

Mean climate response. Modeled annual mean (upper panel) surface air temperature response and (low panel) precipitation response for S50−CTRL (left) and S50-EFF30-CTRL (right). All anomalies shown exceed 95% significance level based on two-sample t test. S50-EFF30 means the conversion efficiency of solar panels is set as a highly idealized 30% (from originally 15%), hence the *effective albedo* equals 0.1+0.30*(1–0.1) = 0.370. By implementing this *effective albedo* in S50-EFF30, the model shows local and global responses are sensitive to albedo change (by comparing left and right column): the local warming anomalies are partly replaced by local cooling anomalies surrounding North Africa, hence less intensified precipitation and cloud cover, and, in turn, roughly opposite but weakened global impacts.

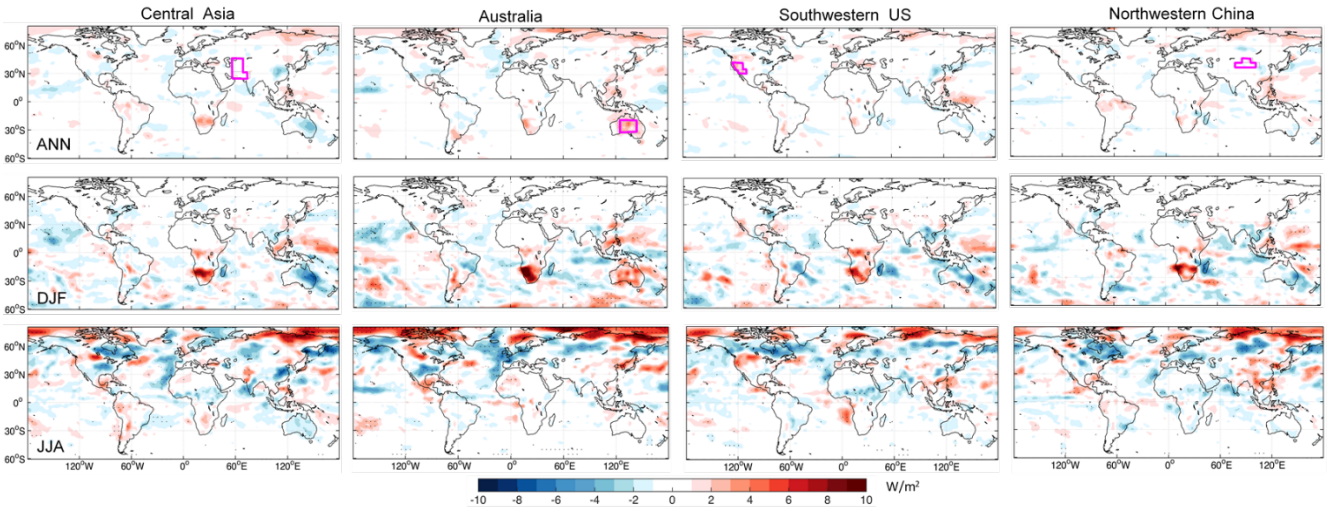

Supplementary Figure 8

(Upper panel) annual mean, (middle panel) DJF mean and (bottom panel) JJA mean of RSDS response in four additional solar farm scenarios. Black dots depict anomalies that exceed 95% significance of *t* test. The location of solar farms in Central Asia, Central Australia and Southwestern USA, Northwestern China are shown by purple polygons (upper panel) and cover 50% of the model gridcells within each polygon.

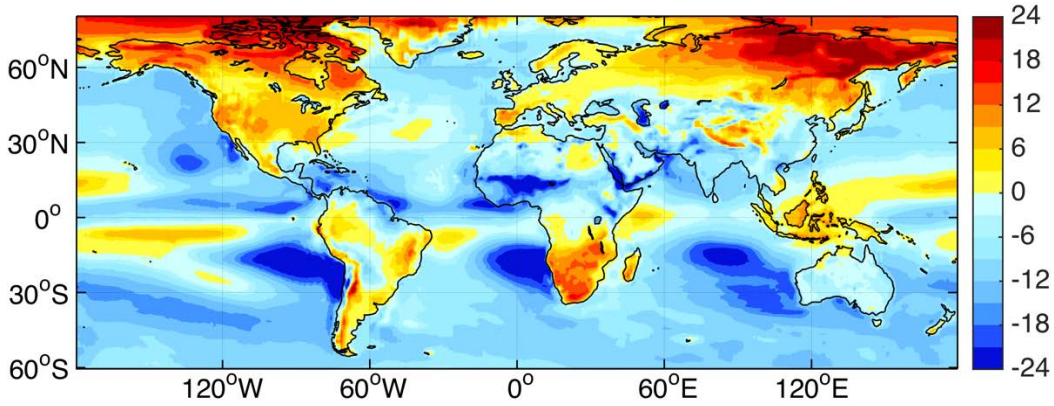

Supplementary Figure 9

The difference of simulated annual mean total cloud cover (%) compared to observation (CERES dataset, https://ceres.larc.nasa.gov/). Except for a strip of the southwestern Sahara, the deviation of simulated cloud cover the tropical regions is generally below 10%. Outside the tropics towards the mid-latitude, the deviation in the US region reaches about 10%. Cloud cover deviations in Europe, Central Asia, East Asia, and Australia are generally within 5%.

		Global (land)	Europe	Asia	N America	Latin America	Africa	Oceania
CTRL	ANN	0.203	0.137	0.221	0.166	0.224	0.250	0.241
	DJF	0.185	0.040	0.164	0.070	0.237	0.235	0.283
	JJA	0.217	0.219	0.265	0.252	0.205	0.252	0.187
S05 - CTRL	ANN	-0.065%	+0.200%	-0.100%	-0.400%	+0.100%	-0.139%	-0.283%
	DJF	+0.021%	+0.099%	+0.086%	+0.038%	-0.272%	+0.287%	-0.328%
	JJA	-0.186%	-0.031%	+0.018%	-0.533%	+0.194%	-0.415%	-0.594%
S20 - CTRL	ANN	-0.493%	-0.200%	-0.500%	+0.100%	+0.500%	-1.589%	-0.339%
	DJF	-0.338%	-0.777%	-0.166%	-0.573%	-0.157%	-0.587%	-0.647%
	JJA	-0.588%	-0.228%	-0.602%	+0.136%	+1.202%	-2.308%	-0.855%
S50 - CTRL	ANN	-1.427%	-1.300%	-1.500%	-0.400%	+1.400%	-4.370%	-0.626%
	DJF	-0.896%	-1.569%	-0.656%	-0.943%	+0.009%	-2.058%	-1.224%
	JJA	-1.733%	-1.276%	-1.403%	-0.165%	+2.588%	-6.255%	-0.591%

Supplementary Table 1

PVpot and its annual (ANN), and DJF, JJA changes averaged over the global landmass and each habitable continent.

		China	USA	Japan	India	Germany	Italy	Australia	Spain	Korea	Vietnam
CTRL	ANN	0.209	0.190	0.168	0.230	0.136	0.182	0.244	0.194	0.181	0.195
	DJF	0.146	0.109	0.115	0.207	0.048	0.086	0.099	0.099	0.132	0.160
	JJA	0.257	0.264	0.214	0.222	0.227	0.281	0.288	0.288	0.214	0.204
S05 - CTRL	ANN	-0.082%	-0.330%	-0.167%	-0.324%	-0.525%	+0.136%	+0.040%	+0.040%	-0.349%	+0.856%
	DJF	+0.091%	+0.179%	-0.852%	-0.368%	-0.013%	+0.481%	+0.562%	+0.562%	-1.240%	+0.154%
	JJA	+0.035%	-0.296%	+0.483%	+0.013%	-0.414%	-0.188%	-0.066%	-0.066%	+1.008%	+1.561%
S20 - CTRL	ANN	-0.281%	+0.201%	-0.669%	-1.291%	-0.940%	-0.826%	-0.331%	-0.331%	-0.444%	-0.453%
	DJF	+0.372%	-0.487%	-0.218%	-0.440%	-2.585%	-0.258%	+0.218%	+0.218%	-0.291%	-2.018%
	JJA	-0.260%	+0.377%	-0.857%	-2.238%	-0.051%	-1.068%	-0.828%	-0.828%	-0.342%	+0.728%
S50 - CTRL	ANN	-1.003%	-0.003%	-1.148%	-2.872%	-2.646%	-2.144%	-0.236%	-0.236%	-2.384%	-1.594%
	DJF	-0.068%	-0.899%	+0.284%	-0.585%	-4.277%	-0.954%	+0.529%	+0.529%	-0.367%	-5.129%
	JJA	-0.762%	+0.429%	-0.027%	-6.286%	-2.843%	-3.112%	-1.375%	-1.375%	-2.197%	+1.026%

Supplementary Table 2

PVpot and its annual (ANN), and DJF, JJA changes averaged over top 10 countries with highest solar power electricity generation (source: https://www.irena.org/Data/View-data-by-topic/Capacity-and-Generation/Country-Rankings).